OUT-OF-OVEN CURING OF POLYMERIC COMPOSITES VIA RESISTIVE MICROHEATERS COMPRISED OF ALIGNED CARBON NANOTUBE NETWORKS

OUT-OF-OVEN CURING OF POLYMERIC COMPOSITES VIA RESISTIVE MICROHEATERS COMPRISED OF ALIGNED CARBON NANOTUBE NETWORKS

Jeonyoon Lee[1*], Itai Y. Stein[1], Erica F. Antunes[2], Seth S. Kessler[3], and Brian L. Wardle[2]

[1]Department of Mechanical Engineering, Massachusetts Institute of Technology
77 Massachusetts Avenue, Cambridge, Massachusetts 02139, United States

[2]Department of Aeronautics and Astronautics, Massachusetts Institute of Technology
77 Massachusetts Avenue, Cambridge, Massachusetts 02139, United States

[3]Metis Design Corporation
205 Portland Street, Boston, Massachusetts 02114, United States

Keywords: Carbon nanotubes, Resistive heating, Polymer composites, Manufacturing, Out-of-autoclave

ABSTRACT

The broader adoption of composite materials in next-generation aerospace architectures is currently limited by the geometrical constraints and high energy costs of traditional manufacturing techniques of PMCs such as autoclave and vacuum-bag-only oven curing techniques. Here, an *in situ* curing technique for PMCs using a resistive heating film comprised of an aligned carbon nanotube (A-CNT) network is presented. A carbon fiber reinforced plastic (CFRP) prepreg system is effectively cured via a single-side CNT network heater incorporated on the outer surface of the laminate without using an autoclave. Evaluation of the curing efficacy shows that composites cured by A-CNT film heaters can achieve degrees of cure that are equivalent or better than composites cured by an autoclave. This manufacturing technique enables highly efficient curing of PMCs while adding multifunctionality to finished composites.

1 INTRODUCTION

Polymer matrix composites (PMCs), especially carbon-fiber-reinforced plastic (CFRP) composites, are widely used as structural materials because of their exceptional physical properties and multifunctionality. Although there are several manufacturing processes for curing PMCs using external stimuli such as heat [1–5] and light [2–4], autoclave curing remains the industrial standard technique for achieving PMCs with the desired properties. In the traditional autoclave manufacturing technique, PMCs are subjected to high temperatures for polymer crosslinking, and high pressure for high fiber volume fraction and low void content. However, manufacturing via autoclave is accompanied by high initial installation costs as well as operating costs of a high temperature pressurized vessel. Most importantly, since an autoclave has size and shape constraints on PMC components, and effective energy transfer for curing is restricted by the indirect heat transfer mechanism via convection of a gas medium inside the vessel, the autoclave manufacturing technique cannot meet the demand for manufacturing flexibility required by state of the art PMCs. Also, the amount of energy for curing composites scales with the size of the component, and is limited by the capacity of autoclave because of fixed volume of gas medium inside of vessel. Thus, the autoclave manufacturing process consumes a fixed amount of energy no matter how large or small the components are. Even an alternative manufacturing technique using microwave heating has the similar drawbacks related in the size and shape constraints due to radiation shielding [6]. Therefore, much interest in new manufacturing technology for PMC has developed.

Here we utilize A-CNT networks as a heating element for a new manufacturing technology (called “out-of-oven”) that eliminates the need of an autoclave for the thermal processing of PMCs. The recent studies on A-CNT networks indicated that re-oriented A-CNT network made via roller

densification are highly scalable [7, 8], and have tunable electron transport properties [7, 9–11]. In addition, since A-CNT network have very low density [9] compared to metal materials, because of the intrinsic density and volume fraction of CNT network [8], A-CNT network based microheaters are suitable for applications requiring a lightweight heating element, such as an anti/deicing system for airplane wings [12]. Thus, using such an A-CNT film heater, we show that PMCs can be effectively and efficiently cured outside an autoclave or oven.

2 MATERIALS AND EXPERIMENTAL

2.1 SYNTHESIS OF ALIGNED CNT ARRAYS AND FILM

Vertically aligned CNT arrays were grown in a 44mm internal diameter quartz tube furnace at atmospheric pressure with a thermal chemical vapor deposition (CVD) process [13, 14]. The CNTs were grown on 40mm x 50mm Si substrates with catalytic layer of 10nm/1nm of Al_2O_3/Fe respectively deposited by electron-beam evaporation. The 40mm x 50mm Si substrate placed in the middle of the quartz tube furnace were first annealed at 680°C under a flow of 1040 sccm of hydrogen gas in order to form nano-particle catalyst. Then, 400 sccm of ethlylene gas was injected into the furnace as the carbon source. The length of CNTs was controlled by changing the time of ethylene gas insertion. In order to obtain better electrical conductivity after densification [7] and enable more electric energy to be dissipated as thermal energy at operating voltage [15], the height of the CNT forests were higher than300 µm. After terminating the insertion of ethylene gas, helium gas was introduced with hydrogen gas in order to weaken bonding between CNT forests and the Si substrate [16] so that the CNT arrays can be easily removed from the substrate. The grown CNTs were reported to have an average outer diameter of ≈7.8 nm (3-7 walls with an average inner diameter of ≈5.1 nm), intrinsic CNT density of ≈1.6 g/cm^3, average inter-CNT spacing of ≈59 nm, and a volume fraction of ≈1.6% CNTs [7, 17, 18]. To produce a film-like material, the vertically grown CNT arrays were densified and reoriented horizontally by using a 10 mm radius rod after covering with a Guaranteed Nonporous Teflon (GNPT) film. Because of the bond-weakening post growth process, the reoriented CNT film was cleanly transferred onto the GNPT film.

2.2 MANUFACTURING OF THE A-CNT HEATER

To utilize an A-CNT film as a heater, two copper mesh electrodes (2CU4-100FA from Dexmet, Inc.) used for lightning strike protection of composite structure were attached to both ends of A-CNT film, ensuring the CNT perpendicular alignment to the length of the electrodes. A-CNT film was held together with the electrodes using a composite surfacing film (TC235-1SF from Tencate Advanced Composite USA, Inc.). In addition to virtual elimination of porosity and imperfections on the composite surface, the surfacing film offers electrical insulation ensuring that electron transport is confined on the A-CNT film, and that proper Joule heating is achieved. A scheme of an A-CNT heater is presented in Figure 1.

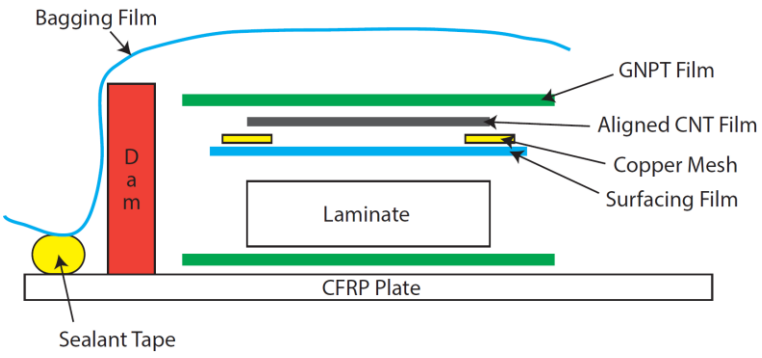

Figure 1: The side view of vacuum bag scheme for curing via an A-CNT film heater [19, 20].

2.3 CURING A COMPOSITE VIA THE A-CNT FILM HEATER

Hexply IM7/8552 pre-impregnated fiber reinforced plastic (prepreg) from Hexcel Corporation was used for the baseline (cured by autoclave) and specimen (cured by A-CNT heater). To minimize the complex heat transfer caused by the orientation of carbon fibers, the curing experiment was performed with a 16-ply unidirectional layup. After laying up, an A-CNT heater was attached onto one side of the uncured laminate as depicted in Figure 2a. The recommended vacuum bag as described in the Hexply 8552 technical data sheet [21] was precisely followed for the baseline specimen, while the air breather was removed from the original vacuum bag arrangement for the specimen with A-CNT heater so that the surface temperature of the A-CNT heater can be measured directly (Figure 2b). For Joule heating of the A-CNT heater, the DC power supply was connected to the two copper mesh electrodes of the A-CNT heater. Input voltage and current were recorded every 300ms during the whole cure cycle using digital multimeters (Hewlett Packard 34401A). Thermography was taken via a thermal camera (PCE-TC 3 from PCE Group, 160 x 120 pixels with range of -10 to 250°C and 0.15°C resolution) every 6s, and the average surface temperature of the CNT film heater in operating region was calculated from the recorded temperature profile. Curing with A-CNT heater was performed by manual adjustment of input voltage ensuring that the average temperature of A-CNT heater matches the provided cure cycle in the technical data sheet. The following cure cycle was used for all curing processes: cure temperature of 225°F with a hold time of 30min; and post cure temperature of 350°F with a hold time of 120min; ramp rate in the range of 3-5°F/min.

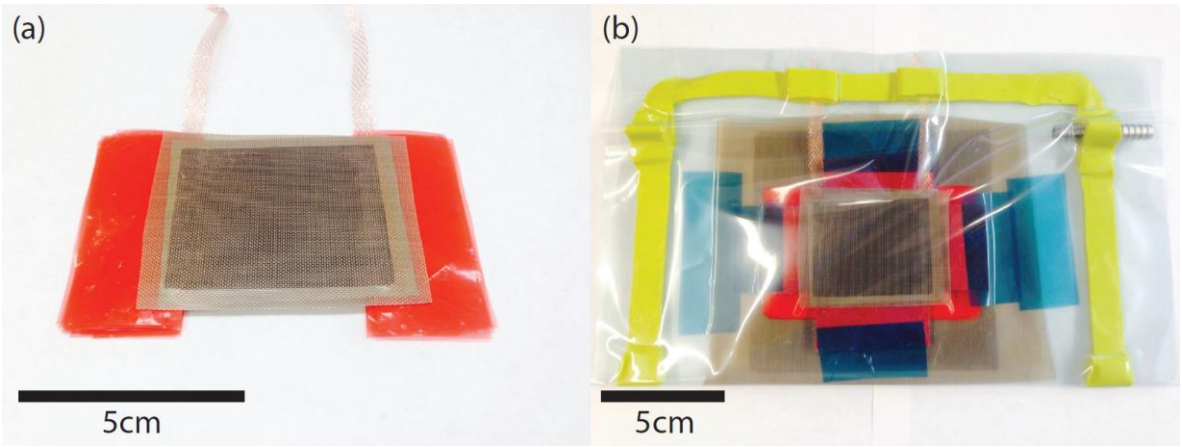

Figure 2: (a) A 16-ply unidirectional layup with A-CNT film heater placed on the surface. (b) A prepared vacuum bag. The red peel plies were inserted at both ends of each layer for delamination after curing to assess the cure state through thickness.

2.4 DEGREE OF CURE ANALYSIS

After thermal processing of the composite, the degree of cure (DoC) was calculated to evaluate whether the thermal energy yielded from A-CNT heater was effectively transferred into the composite. To analyze spatial DoC, differential scanning calorimetry (DSC) was conducted on three delaminated layers among 16 layers (2nd, 7th, and 15th ply of the laminate). In each layer, three regions defined as left, middle, and right area were analyzed additionally to obtain in-plane DoC (see Figure 3). The DoC was calculated by comparing the area of the exothermic peak of the cured laminate to that of the uncured prepreg, after heating up to 300°C at 4°C/min ramp up rate. In this work, the DoC of the uncured prepreg is then defined as 0%, while the DoC of a fully cured laminate is defined as 100%. DSC was conducted with a TA Instruments DISCOVERY DSC under a constant N_2 flow rate of 50mL/min as a purge gas. The amount of cured composite (4-8mg) was used for analysis of each region.

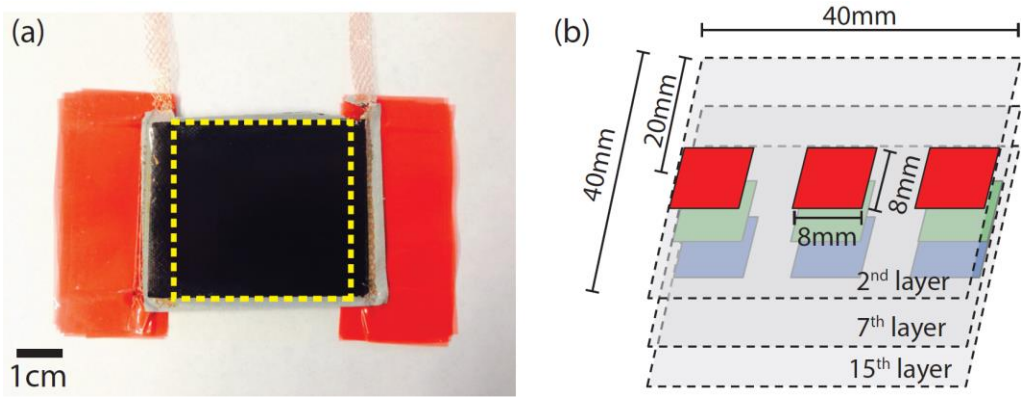

Figure 3: (a) A manufactured composite. (b) Illustration of analyzed regions on 2nd, 7th, and 15th layer [19, 20]. Dashed lines in both figures indicate the operating region of A-CNT film heater.

3 RESULTS AND DISCUSSION

3.1 THERMOGRAPHY AND RESPONSE OF A-CNT FILM HEATER DURING CURING

The temperature of CNT film heater was manually controlled to follow the recommended cure cycle. Figure 4 (a) presents the thermography of A-CNT film heater at an average temperature of 350°F (Initial cure stage). Since the electrical current flowed in the area between the two electrodes, Joule heating occurred in that area with maximum temperature at the center. Since the CNT film heater was not thermally insulated, temperature gradients were observed at the edges of the CNT heater. Also, because the temperature of the A-CNT heater was obtained as an area average of the working region (see the dashed box in Figure 4) where Joule heating occurred, the temperature at the center of the heater was higher than the initial cure temperature. However, the thermal distribution changed after the initial curing region where flow, gelation, and vitrification of polymer occur [22]. Since the rate of polymer infusion into the A-CNT network and gelation varies through the thickness of the A-CNT film heater, the resistance at each region does not change uniformly. Therefore, in order to obtain a uniform resistance change throughout the A-CNT film heater during the initial cure stage, the underlying physics of polymer infusion process into A-CNT network should be explored.

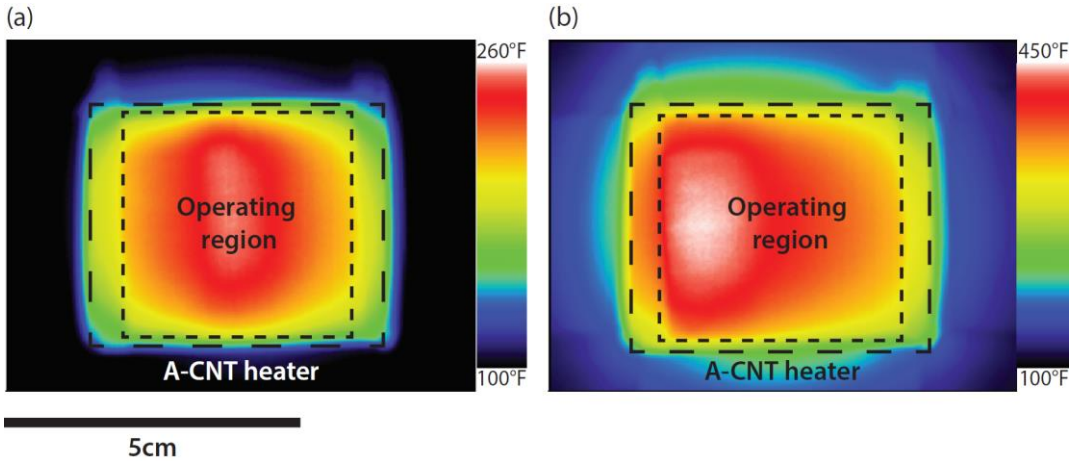

Figure 4: Thermography of the A-CNT film heater. (a) Thermal distribution at the starting point of the initial cure stage (Stage II). (b) Thermograph at the post cure stage (Stage IV). See Figure 5 for the definition of Stages II and Stage IV. Inner dashed box indicates the operating region of heater, and outer box presents the A-CNT heater including electrodes.

Figure 5 presents the thermal response during the cure process illustrating that the temperature of the A-CNT heater followed the specified cure cycle precisely. The electrothermal response of the A-CNT film heater during the cure process consists of five stages as follows: three ramps stages (I, III, and V), an initial cure stage (II) where flow, gelation, and vitrification of polymer occur, and a post cure stage (IV) where polymer crosslinking occurs [22]. In Stage I, where the temperature ramps up from room temperature to 225°F, the resistance of A-CNT heater first decreases from ≈13Ω to ≈11Ω, and then increases to ≈12.5Ω, while power increases from 0W to ≈10.8W. Before reaching the initial cure temperature, the resistance of A-CNT film heater decreases due to negative thermal coefficient of resistance (TCR) of the A-CNT network. Once the temperature reaches the initial cure temperature, the resistance starts to increase because the infusion of polymer into the A-CNT network [23] increases the CNT-CNT junction resistance [24]. In Stage II, temperature is held at 225°F, while the infiltration of polymer in to the A-CNT network continues. The resistance increases from ≈12.5Ω to ≈16.5Ω, while power decreases from ≈10.8W to ≈10.3W. Here, the liquefied polymer transforms to a rubber-like state, and then to a solid glassy state [25]. In stage III, the temperature ramps-up to the post cure temperature of 350°F. Resistance decreases from ≈16.5Ω to ≈15.2Ω because of negative TCR of the A-CNT network similar to Stage I, while power increases from ≈10.3W to ≈24W. In Stage IV, where temperature is maintained at 350°F for the post cure process, the resistance increases from ≈15.2Ω to ≈17.6Ω, and power decreases from ≈24W to ≈20.8W. At this stage, the crosslinking occurs, and the desired mechanical properties of the composite are acquired [22]. Stage V consists of temperature ramp-down after post curing and the resistance increases from ≈17.6Ω to ≈20Ω due to negative TCR.

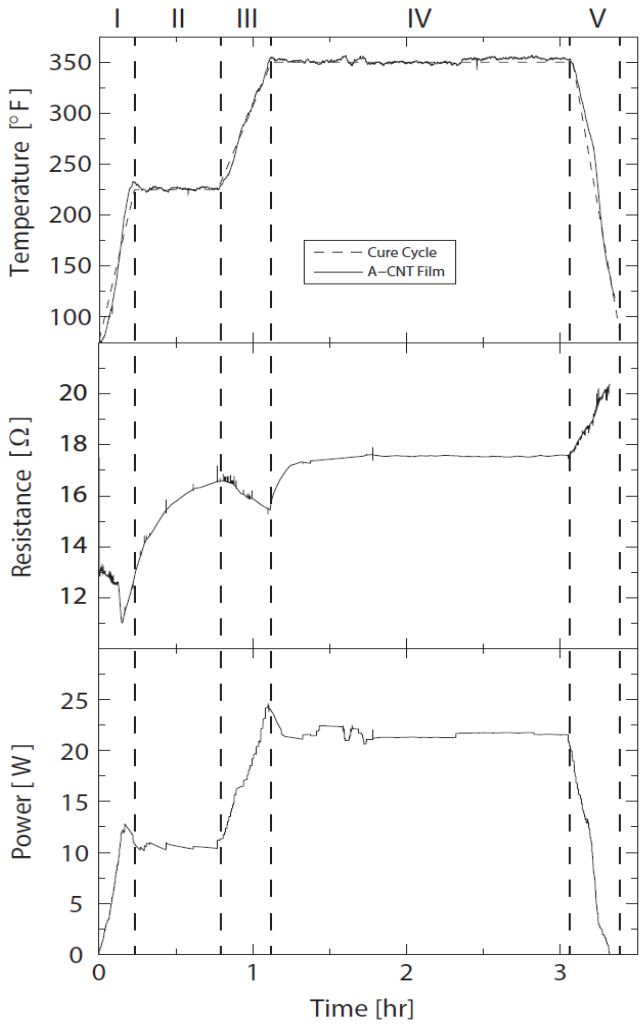

Figure 5: Thermal and electrical response of the A-CNT film heater during curing cycle.

3.2 EVALUATION OF DEGREE OF CURE

To assess the efficacy of the A-CNT film heater for thermal processing of carbon fiber composite, an analysis of the degree of cure was conducted to evaluate the composite quality, since DoC is one of important parameters determining the mechanical properties of a composite [26]. As presented in Figure 6, overall DoCs (≈90%-96%) for the out-of-oven technique are within the range of the DoC evaluated for a baseline composite processed via autoclave (≈92%). Figure 6 (a) shows that the DoC of the layer right below the surface (2nd layer) strongly depends on the surface temperature of the A-CNT film heater. Since the final extent of DoC is limited by the cure temperature [27], uniform thermal distribution within the A-CNT film heater is necessary for the production of composites with uniform quality. Figure 6 (b) illustrates that the average value of DoC in each layer decreases as the distance from the surface (i.e. the layer number) increases. This is because the asymmetric (one-sided heater) and uninsulated setup used here simulate the worst case scenario where heat is conducted from the 1st layer to the 16th layer while suffering significant thermal losses throughout the laminate. Thus, the region closer to the CNT heater shows a higher temperature and respective DoC. Moreover, the spatial variation of the DoC in the composite processed via A-CNT film heater shows good agreement with the thermal distribution within the laminate. Once a uniform thermal distribution is achieved within the A-CNT film heater and thermal insulation is used on the whole vacuum bag setup, out-of-oven curing of composites with homogenous DoCs will become possible.

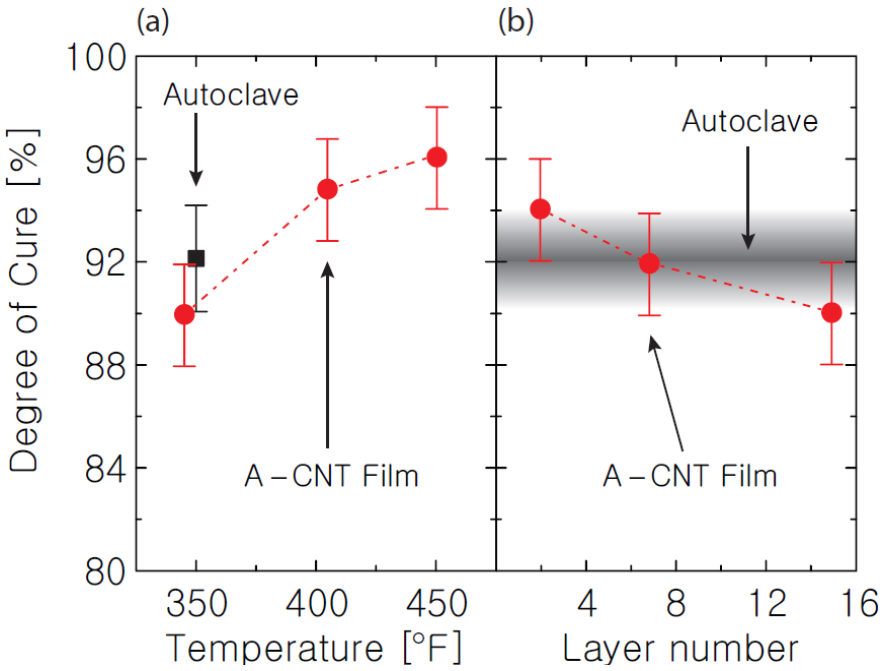

Figure 6: Spatial degree of cure in composite processed in autoclave and out-of-oven technique. (a) The DoCs of the 2nd layer as a function of temperature. Temperature corresponds to the post cure temperature each region, and (b) Average value of the DoCs as a function of layer number. See Figure 4 for the illustration of analyzed region and definition of layer number.

4 CONCLUSIONS

In summary, a new polymer matrix composite processing technique that utilizes a nanostructured resistive heating film comprised of an aligned carbon nanotube (A-CNT) network is reported. The resistive film heater is incorporated into the finished part as a nanocomposite of the surfacing film typically used in finished composite parts. The experimental results show that the carbon fiber reinforced plastic (CFRP) prepreg laminates are effectively cured via a single A-CNT film heater attached to the top surface of the laminate without using an autoclave. The efficacy of this curing method is quantified via a degree of cure (DoC) analysis, which illustrates that the in-plane spatial

variation of the DoC are directly correlated to the maximum temperature of each spot in the laminate during the cure process. Through-thickness spatial variation in the DoC is found to be < 6% for the one-sided curing experiment, and the overall DoC is found to be ~90%, which is the usual DoC for the structural composites. While the A-CNT film heater is shown to be effective for curing the autoclave-designed prepreg material, it is not a solution to the poor interlaminar properties (e.g., high void content) that are generated with the use of vacuum but not pressure. Other materials, such as out-of-autoclave (OoA) or other solutions should be sought. However, compared to conventional curing methods, the use of an A-CNT film for curing may decrease the energy required to cure polymer matrix composites (<25W maximum peak for the A-CNT film heater, >1KW maximum peak for the autoclave), since ~25-50% of total acquisition cost of carbon composites originate from thermal processing [28]. After being used as a heating source for curing, A-CNT film can be integrated into the laminate, adding multifunctionality with potential applications for anti/deicing systems on aerosurfaces. In the future, the underlying physics that govern the electron transport properties of the aligned CNT network should be explored to enable precise control over the A-CNT film heater output power during curing. Integration of these findings into next-generation polymer matrix composite manufacturing techniques may enable real-time curing status sensing, and reduction of total cure cycle through ramp rate optimization.

ACKNOWLEDGEMENTS

This work was supported by Airbus Group, Boeing, Embraer, Lockheed Martin, Saab AB, TohoTenax, and ANSYS through MIT's Nano-Engineered Composite aerospace Structures (NECST) Consortium and was supported by the U.S. Army Research Office under contract W911NF-07-D-0004 and W91NF-13-D-0001. J.L. acknowledges support from the Kwanjeong Educational Foundation. I.Y.S was supported by the Department of Defense (DoD) through the National Defense Science & Engineering Graduate Fellowship (NDSEG) Program. E.F.A. acknowledges support from Brazilian agency for research funding (CNPq), Science without Borders Program. S.S.K. acknowledges support from Naval Sea Systems Command contract N00024-12-P-4069 for SBIR topic N121-058. The authors thank Sunny Wicks (MIT), John Kane (MIT) and the entire necstlab at MIT for technical support and advice. This work made use of the core facilities at the Institute for Soldier Nanotechnologies at MIT, supported in part by the U.S. Army Research Office under contract W911NF-07-D-0004, and was carried out in part through the use of MIT's Microsystems Technology Laboratories.

REFERENCES

[1] Wojtecki, R. J., Meador, M. a & Rowan, S. J. Using the dynamic bond to access macroscopically responsive structurally dynamic polymers. *Nat. Mater.* **10,** 14–27 (2011).

[2] Burattini, S., Greenland, B. W., Chappell, D., Colquhoun, H. M. & Hayes, W. Healable polymeric materials: a tutorial review. *Chem. Soc. Rev.* **39,** 1973–1985 (2010).

[3] Hager, M. D., Greil, P., Leyens, C., Van Der Zwaag, S. & Schubert, U. S. Self-healing materials. *Adv. Mater.* **22,** 5424–5430 (2010).

[4] Hammock, M. L., Chortos, A., Tee, B. C. K., Tok, J. B. H. & Bao, Z. 25th anniversary article: The evolution of electronic skin (E-Skin): A brief history, design considerations, and recent progress. *Adv. Mater.* **25,** 5997–6038 (2013).

[5] Yan, X., Wang, F., Zheng, B. & Huang, F. Stimuli-responsive supramolecular polymeric materials. *Chem. Soc. Rev.* **41,** 6042-6065 (2012).

[6] Thostenson, E. T. & Chou, T.-W. Microwave processing: fundamentals and applications. *Compos. Part A Appl. Sci. Manuf.* **30,** 1055–1071 (1999).

[7] Lee, J., Stein, I. Y., Devoe, M. E., Lewis, D. J., Lachman, N., Kessler, S. S., & Wardle, B. L. Impact of carbon nanotube length on electron transport in aligned carbon nanotube networks. *Appl. Phys. Lett.* **106,** 053110 (2015).

[8] Stein, I. Y. & Wardle, B. L. Morphology and processing of aligned carbon nanotube carbon matrix nanocomposites. *Carbon N. Y.* **68,** 807–813 (2014).

[9] Zhang, L., Zhang, G., Liu, C. & Fan, S. High-density carbon nanotube buckypapers with superior transport and mechanical properties. *Nano Lett.* **12,** 4848–4852 (2012).

[10] Chen, G., Futaba, D. N., Sakurai, S., Yumura, M. & Hata, K. Interplay of wall number and diameter on the electrical conductivity of carbon nanotube thin films. *Carbon.* **67,** 318–325 (2014).

[11] Marschewski, J., In, J. Bin, Poulikakos, D. & Grigoropoulos, C. P. Synergistic integration of Ni and vertically aligned carbon nanotubes for enhanced transport properties on flexible substrates. *Carbon N. Y.* **68,** 308–318 (2014).

[12] Buschhorn, S. T., Lachman, N., Gavin, J., Wardle, B. L., Kessler, S. S., & Thomas, G. Electrothermal Icing protection of Aerosurfaces Using Conductive Polymer Nanocomposites. *AIAA* (2013).

[13] Wardle, B. L., Saito, D. S., García, E. J., Hart, A. J., de Villoria, R. G., & Verploegen, E. A. Fabrication and Characterization of Ultrahigh-Volume- Fraction Aligned Carbon Nanotube-Polymer Composites. *Adv. Mater.* **20,** 2707–2714 (2008).

[14] Marconnet, A. M., Yamamoto, N., Panzer, M. A., Wardle, B. L. & Goodson, K. E. Thermal Conduction in Aligned Carbon Nanotube–Polymer Nanocomposites with High Packing Density. *ACS Nano* **5,** 4818–4825 (2011).

[15] Janas, D. & Koziol, K. K. Nanoscale A review of production methods of carbon nanotube and graphene thin fi lms for electrothermal applications. *Nanoscale* **6,** 3037–3045 (2014).

[16] Mitchell, R. R., Yamamoto, N., Cebeci, H., Wardle, B. L. & Thompson, C. V. A technique for spatially-resolved contact resistance-free electrical conductivity measurements of aligned-carbon nanotube/polymer nanocomposites. *Compos. Sci. Technol.* **74,** 205–210 (2013).

[17] Hart, A. J. & Slocum, A. H. Rapid Growth and Flow-Mediated Nucleation of Millimeter-Scale Aligned Carbon Nanotube Structures from a Thin-Film Catalyst Rapid Growth and Flow-Mediated Nucleation of Millimeter-Scale Aligned Carbon Nanotube Structures from a Thin-Film Catalyst. *J. Phys. Chem. B* **110,** 8250-8257 (2006).

[18] Stein, I. Y., Lachman, N., Devoe, M. E. & Wardle, B. L. Exohedral physisorption of ambient moisture scales non-monotonically with fiber proximity in aligned carbon nanotube arrays. *ACS Nano* **8,** 4591–4599 (2014).

[19] Lee, J. In situ curing of polymeric composites via resistive heaters comprised of aligned carbon nanotube networks. Massachusetts Institute of Technology. (2014).

[20] Lee, J., Stein, I. Y., Kessler, S. S. & Wardle, B. L. Aligned Carbon Nanotube Film Enables Thermally Induced State Transformations in Layered Polymeric Materials. *ACS Appl. Mater. Interfaces* **7**, 8900-8905 (2015). doi:10.1021/acsami.5b01544

[21] Hexcel Corporation. HexPly 8552 Epoxy Matrix Product Data. <http://www.hexcel.com/Resources/DataSheets/Prepreg-Data-Sheets/8552_us.pdf>

[22] Centea, T., Grunenfelder, L. K. & Nutt, S. R. A review of out-of-autoclave prepregs – Material properties, process phenomena, and manufacturing considerations. *Compos. Part A Appl. Sci. Manuf.* **70,** 132–154 (2015).

[23] García, E. J., Hart, a J., Wardle, B. L. & Slocum, A. H. Fabrication of composite microstructures by capillarity-driven wetting of aligned carbon nanotubes with polymers. *Nanotechnology* **18,** 165602 (2007).

[24] Qiu, J., Terrones, J., Vilatela, J. J., Vickers, M. E., Elliott, J. A., & Windle, A. H. Liquid infiltration into carbon nanotube fibers: Effect on structure and electrical properties. *ACS Nano* **7,** 8412–8422 (2013).

[25] Ur, K. & Vora, R. Mechanical Properties Evolution During Cure for Out-of-Autoclave Carbon-Epoxy Prepregs. *J. Appl. Polym. Sci.* **132,** 41548 (2012).

[26] Lee, S. Y. & Springer, G. S. Effects of Cure on the Mechanical Properties of Composites. *J. Compos. Mater.* **22 ,** 15–29 (1988).

[27] Yousefi, A., Lafleur, P. G. & Gauvin, R. Kinetic Studies of Thermoset Cure Reactions : A Review. *Polym. Compos.* **18,** 157–168 (1997).

[28] Eaglesham, M. A. A decision support system for advanced composites manufacturing cost estimation. Virginia Polytechnic Institute and State University. (1998).